

Ferroelectric-Specific Stark Effect in Stoichiometric $\text{LiNbO}_3\text{:Fe}$ at Room Temperature

S. A. Basun,¹ V. E. Bursian,¹ D. R. Evans,² A. A. Kaplyanskii,¹ A. G. Razdobarin,¹ and L. S. Sochava¹

¹*A.F. Ioffe Physico-Technical Institute, RAS, 194021 St. Petersburg, Russia*

²*Air Force Research Laboratory, Materials and Manufacturing Directorate, Wright-Patterson Air Force Base, Ohio 45433, USA*

(Received 6 July 2007; published 6 February 2008)

By means of EPR spectroscopy of $\text{LiNbO}_3\text{:Fe}$ at room temperature (RT) it is shown that the Stark effect in ferroelectric crystals can be different from that observed in other materials. Novel properties appear when an external E field reverses the direction of the spontaneous polarization, the direction of the linear Stark shift stays the same with a reversal of the E field. The corresponding spectral line shifts can occur over a long time scale (hours). These properties seem to be a general feature of the Stark effect in ferroelectric crystals when the external E field exceeds the coercive field.

DOI: [10.1103/PhysRevLett.100.057602](https://doi.org/10.1103/PhysRevLett.100.057602)

PACS numbers: 77.80.Fm, 76.30.Fc, 77.84.Dy

The Stark effect observed in the optical and radio frequency spectra of crystals with point defects is known to have either a quadratic or linear E field dependence. When a dipole moment of the defect center (hereafter—center) is induced *only* by an external electric field, the spectral line shifts are proportional to the square of the applied E field, and the direction of the shifts does not depend on polarity of the E field. In a linear Stark effect, the dipole moment of the center is already induced by the polar axial component of the crystal field; the direction of the linear-in-field spectral shifts reverses upon a change in polarity of the external E field. A review on the Stark effect in crystals is given in Ref. [1]. The goal of this Letter is to demonstrate that manifestations of the Stark effect in ferroelectric crystals can become quite different when the external E field exceeds the coercive field at a given temperature and switches the spontaneous polarization of the sample, which consequently reverses the direction of the polar axis of the center given by the direction of the polar axis of the crystal. This reversal effect causes the direction of the linear Stark shifts to be independent of the external E field polarity. The Stark effect is neither quadratic nor linear but *linear in absolute magnitude* with dynamics that reveals the repolarization of the ferroelectric crystal. Below the coercive field, when repolarization cannot occur, only a standard linear Stark effect is observed. Parallel measurements of the repolarization currents allowed us to confidently assign the observed peculiarities to the ferroelectric properties of the sample.

Ferroelectric-specific properties of the Stark effect are found in the electron paramagnetic resonance (EPR) spectra of $\text{LiNbO}_3\text{:Fe}$ crystals. EPR spectra were measured over the temperature range from 300 to 78 K on an X-band conventional EPR spectrometer. E fields up to 5 kV/mm were applied to c -cut plates of $\text{LiNbO}_3\text{:Fe}$, $3.8 \times 5.8 \times 1.0 \text{ mm}^3$. Opposite c faces were coated with aquadag electrodes and the current was measured in the circuit with an electrometer. LiNbO_3 samples with compositions close to being stoichiometric were studied ($\text{LiNbO}_3\text{:0.1 mol. \%Fe}_2\text{O}_3$). These were cut from a con-

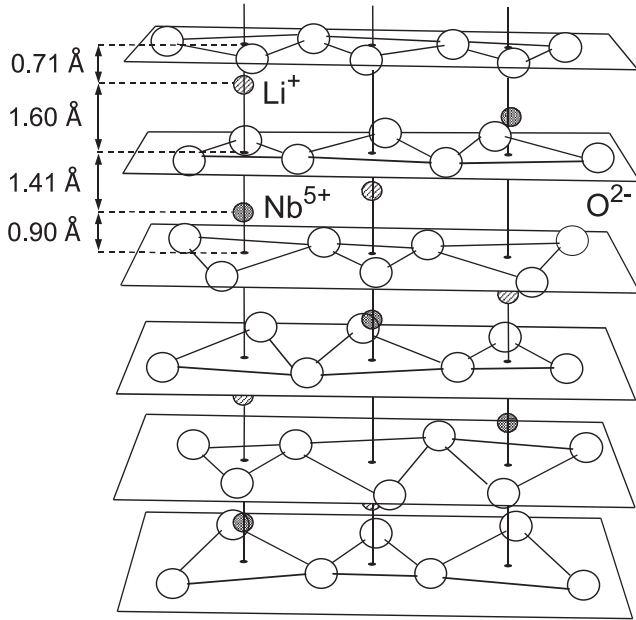
gruently grown boule and subjected to a vapor transport equilibration (VTE) procedure at the University of Osnabrück, Germany, to improve the stoichiometry [2].

An Fe^{3+} center with the $\text{Fe}^{3+}[\text{Nb}]\text{-K}^+$ structure has been found in Refs. [3,4], where the stoichiometry of the samples studied was improved by the addition of K_2O to the melt. In our samples, which have been grown without potassium, a center with very close spin-Hamiltonian parameters appeared after VTE processing. Li ions are known to enter the sample during VTE treatment [2], with a majority of them filling Li-vacancies inherent to congruent LiNbO_3 ; although in principle some of the Li ions can occupy a structural vacancy next to a $\text{Fe}^{3+}[\text{Nb}]$ ion. This results in a reasonable assignment of the center studied in this work to the $\text{Fe}^{3+}[\text{Nb}]\text{-Li}^+$ structure (Fe^{3+} in a Nb site with an irregular Li^+ ion on the c axis) [5].

Li^+ and Nb^{5+} ions in oxygen octahedra are shifted along the c axis from the center of the octahedra (Fig. 1). The lack of inversion site symmetry allows a *linear* Stark effect on the spectral lines of Fe ions, for either $\text{Fe}^{3+}[\text{Li}^+]$ or $\text{Fe}^{3+}[\text{Nb}^{5+}]$ centers. In LiNbO_3 , a linear Stark effect has been observed in nuclear quadrupole resonance (NQR) on ^{93}Nb [6] and in optical absorption spectra of Cr^{3+} [7].

In this work, a measurable Stark effect is found only on the EPR lines of the $\text{Fe}^{3+}[\text{Nb}]\text{-Li}^+$ center. Figure 2 shows the effect of the external E field, $E \parallel c$, on the resonant magnetic field of the $M = 1/2 \leftrightarrow 3/2$ transition. Similar results are obtained on other lines of the $\text{Fe}^{3+}[\text{Nb}]\text{-Li}^+$ center.

At $T = 100 \text{ K}$ repolarization of our samples under the employed E fields does not occur (see below), and a typical linear Stark effect is observed [Fig. 2(a)]; the direction of the shift reverses with a reversal of the E field—this is also the case with the NQR results of [6]. At RT the threshold field needed to repole LiNbO_3 (coercive field) can be as low as 0.8 kV/mm for stoichiometric samples [8], and ferroelectric manifestations can be encountered. Indeed, the behavior of the Stark effect becomes quite different—see Fig. 2(b); together with immediate spectral changes, a long term evolution is observed upon a reversal of the E

FIG. 1. Crystal lattice of LiNbO_3 in the ferroelectric phase.

field. The closed circles and triangles in Fig. 2(b) show the steady-state position of the EPR line as a function of the applied E field. Varying a positive E field applied in the direction of the spontaneous polarization of the crystal (as determined with pyroelectric measurements by heating the sample and measuring the polarity of the voltage generated across the sample), we only observe the usual instantaneous linear Stark shifts of the EPR line [solid triangles on Fig. 2(b)]. Switching of the E field to -3.5 kV/mm results in an instantaneous (arrow 1) and subsequent gradual (open circles and arrow 2) shifts of the EPR line. Further varying of negative E field causes only an instantaneous linear-in-field shift of the resonance line [solid circles on Fig. 2(b)]. Immediate and slow spectral changes caused by the reversal of the E field from a negative value to $+3.5$ kV/mm are indicated by the arrows 3 and 4, respectively. We find [Fig. 2(b)] that at $T = 300$ K the Stark effect gains new characteristics: (i) the steady-state shifts are still linear-in-field, but the EPR line shifts to a higher magnetic field for *both* polarities of the external E field, (ii) for a *zero* E field, *two* different positions of the same EPR line can be observed, before and after subjecting the sample to an E field of the opposite polarity.

Characteristic (i).— Fig. 3 gives a deeper insight to the issue and helps elucidating the ferroelectric origin of the novel characteristics of the Stark effect at RT. An E field, $E \parallel c$, with opposite polarities was applied to the sample [Fig. 3(a)]; the dynamics of the Stark shift [Fig. 3(b)] was measured in parallel with the repolarization current [Fig. 3(c)]. With the voltage applied across the sample in the direction of its spontaneous polarization, repoling cannot occur, and only short spikes of current in the circuit can

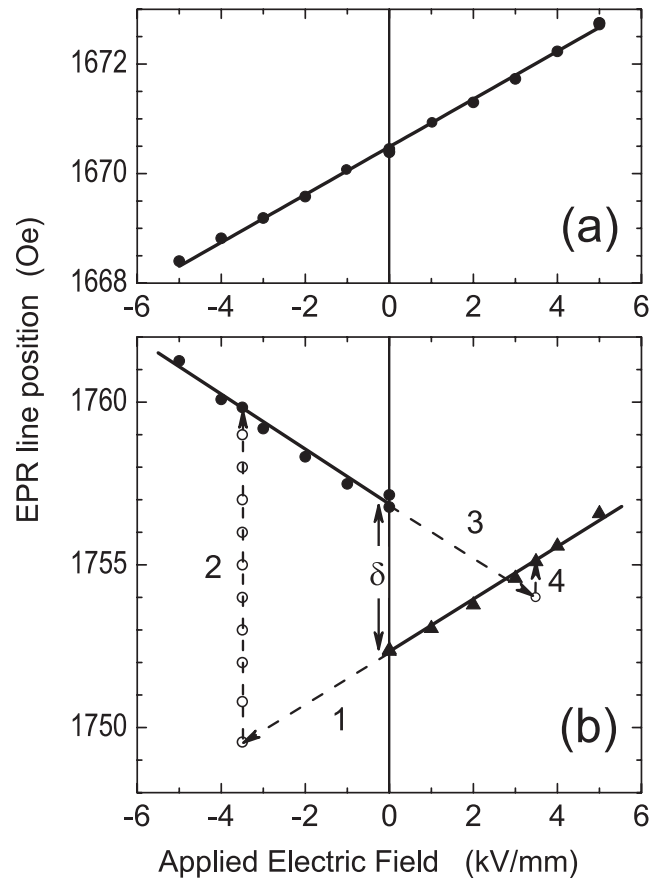


FIG. 2. Stark effect on the EPR line $M = 1/2 \leftrightarrow 3/2$ of the $\text{Fe}^{3+}[\text{Nb}]\text{-Li}^+$ center in LiNbO_3 . Closed circles and triangles: steady-state positions of the line. Open circles: transients in the course of repoling [see region 2 in Fig. 3(b)]. Arrows 1, 3 and 2, 4 indicate the immediate and slow spectral changes, respectively. $E \parallel H \parallel c$. $T = 100$ K (a) and 295 K (b).

be observed [Fig. 3(c)] due to the recharging of the capacitance of the sample and the lead wires. The dark current was negligible (smaller than the noise level (<10 pA)).

At RT, the reversal of the external E field makes it opposite to the direction of the spontaneous polarization, which may start repoling the sample. A long transient current is observed, see Fig. 3(c); integration of the current is displayed in Fig. 3(d). The transferred charge density, $Q = 117 \pm 2 \mu\text{C cm}^{-2}$, is in agreement with double the value of the spontaneous polarization ($2P_s$) of LiNbO_3 : $P_s = 50\text{--}70 \mu\text{C cm}^{-2}$ [9,10]; this is clear evidence that at RT an E field of 3.5 kV/mm does switch the polarization of our samples. The dynamics of the measured repolarization is the same as that of the slow shift of the EPR line [region 2 in Fig. 3(b)], hence the novel manifestations of the Stark effect shown in Figs. 2(b) and 3(b) are caused by repolarization of the sample.

It is worth noting that repolarization current was not detected at 100 K, the repolarization current density at $E = 6$ kV/mm was certainly smaller than 50 pA cm^{-2} . This

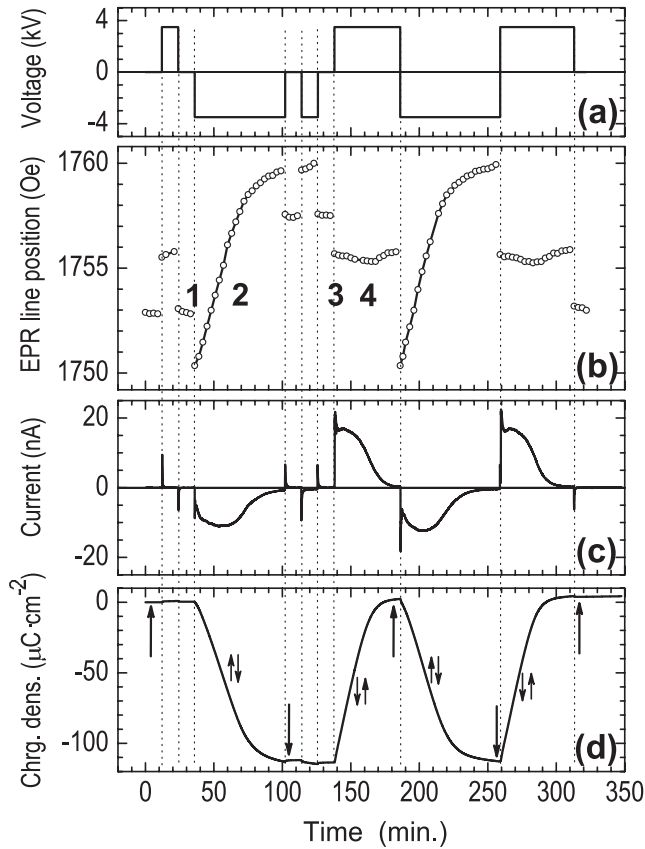


FIG. 3. Simultaneously measured dynamics of the $M = 1/2 \leftrightarrow 3/2$ transition: (a) switching of the external electric field polarity, $E \parallel c$; (b) EPR line position; (c) poling current; and (d) poling charge density. The arrows show the change of the polarization in the course of repoling of the sample. Labels 1–4 in (b) correspond to the arrows 1–4 in Fig. 2(b). $E \parallel H \parallel c$, $T = 295$ K, 9.3 GHz.

means that switching time period at 100 K is at least a month long, which is 3 orders of magnitude longer than the time scale of our EPR experiments. An increase in the coercive field at lower temperatures is expected in LiNbO_3 since it is known that it significantly decreases when heated above RT; see Ref. [11].

It is the repoling of the monodomain sample that provides a clear explanation to the V-shaped characteristic of the Stark effect at RT shown in Fig. 2(b). The direction of the polar axis of the center is given by the direction of the polar axis (c axis) of the sample. When an opposite polarity electric field \mathbf{E} reverses the direction of the polar axis \mathbf{c} (in fact, it reverses the monodomain sample as a whole), the direction of the polar asymmetry of the center reverses along with the sign of the dipole moment \mathbf{d} of the $M = 1/2 \leftrightarrow 3/2$ transition. As a result, the direction of the linear Stark shift, $\mathbf{d} \cdot \mathbf{E}$, does not change: the EPR line shifts to a higher magnetic field regardless the E field polarity, i.e., V-shaped characteristic.

In the course of repoling, the sample consists of domains with opposite directions of spontaneous polarization, parallel and antiparallel to the external E field [schematically shown with arrows in Fig. 3(d)]. In the external field, positions of the spectral line are different in opposite domains; the resulting EPR line becomes a sum of the two lines. The shift between the lines in the course of the $+3.5 \rightarrow -3.5$ kV repoling [arrow 2 in Fig. 2(b)] is ~ 10 Oe—significantly smaller than their width ~ 60 Oe; therefore, they cannot be resolved. (Such a large linewidth with a negligible dependence on temperature usually suggests an inhomogeneous character of the broadening caused by slightly different environments of the centers. At the same time, a significant or even dominating contribution of an unresolved superhyperfine structure should not be ruled out for a high quality and stoichiometric sample.) It is known in spectroscopy that redistribution of the intensity between the components of an unresolved doublet line causes a shift of the doublet. In our case, this shift must be proportional to the time-dependent volume fraction of the antiparallel domains (ranging from 1 to 0) in the course of the repoling. If the slow Stark shifts are indeed caused by the repolarization, then—due to this linear relationship—the dynamics of these two processes must be identical. This is exactly the case how they appear in region 2 in Figs. 3(b) and 3(c).

Characteristic (ii).—Figs. 3(c), 3(d), and 2(b) show that the dynamics of repolarization in opposite directions is nearly the same—but the slow changes of the EPR line position are much stronger when the E field is switched from $+3.5$ to -3.5 kV/mm [compare regions 2 and 4 in Fig. 3(b) and arrows 2 and 4 in Fig. 2(b)]. This difference is caused by the structure of the $\text{Fe}^{3+}[\text{Nb}]\text{-Li}^+$ center, namely, the presence of a stable defect (an irregular Li^+ ion) close to the Fe^{3+} ion.

Figure 4 shows a section of the crystal lattice around the $\text{Fe}^{3+}[\text{Nb}]\text{-Li}^+$ center before and after repoling. In the course of repoling, Nb^{5+} ions are shifted by $\Delta_{\text{Nb}} = 0.51$ Å along the c axis (see the arrow in Fig. 4 (right)) from one oxygen plane to the other, although they remain within the same oxygen octahedron. This is also the case for Fe^{3+} (see Fig. 4) whose ionic radius is similar to that of Nb^{5+} , 0.8 Å (Ref. [12]). Unlike Nb^{5+} ions, Li^+ ions hop by $\Delta_{\text{Li}} = 1.42$ Å through the oxygen plane to corresponding structural vacancies: this is proved by a straightforward evaluation of the corresponding displacement charge density $Q = (e\Delta_{\text{Li}} + 5e\Delta_{\text{Nb}})n$, where $n = 1.87 \times 10^{22} \text{ cm}^{-3}$ is a concentration of Li^+ and Nb^{5+} ions in LiNbO_3 , and e is the electron charge. We obtain $Q = 119 \mu\text{C cm}^{-2}$, which is in excellent agreement with the value $Q = 2P_s = 117 \pm 2 \mu\text{C cm}^{-2}$ measured in this work.

Hopping through the oxygen plane is not possible for Li^+ ions located close to Fe^{3+} (ions 1 and 2 in Fig. 4); the “destination” oxygen octahedra are occupied either by an Fe^{3+} ion or by a Li^+ ion 1. Li^+ ions 1 and 2 remain in their

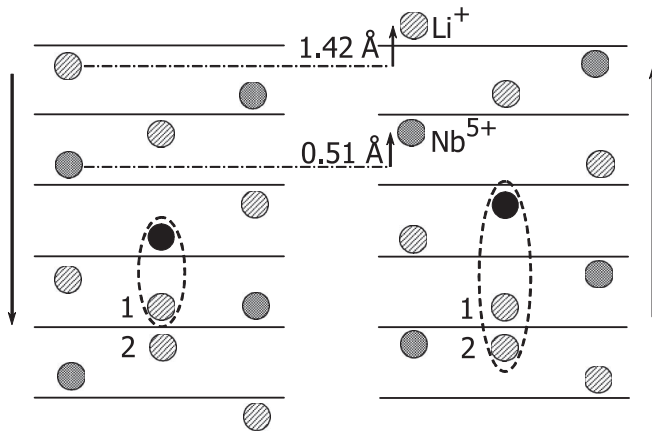


FIG. 4. Transformation of the $\text{Fe}^{3+}[\text{Nb}]\text{-Li}^+$ center under repoling of LiNbO_3 : structures of the center before repoling (left) and after repoling (right). The displacements of the Li^+ and Nb^{5+} sublattices are shown by arrows. Solid horizontal lines: oxygen planes. Black circles: Fe^{3+} ion. The longer arrows indicate the directions of the spontaneous polarization.

oxygen octahedra before and after repoling. It is seen in Fig. 4 that the sample before repoling [Fig. 4 (left)] has an irregular Li^+ ion 1 occupying the site next to the $\text{Fe}^{3+}[\text{Nb}^{5+}]$ oxygen octahedron; Li^+ ion 2 is a regular ion. After repoling [Fig. 4 (right)], Li^+ ion 1 becomes a regular ion, but Li^+ ion 2 now occupies a structural vacancy (the next nearest vacancy to the $\text{Fe}^{3+}[\text{Nb}^{5+}]$ oxygen octahedron).

Before and after the repoling of the sample, the $\text{Fe}^{3+}[\text{Nb}]\text{-Li}^+$ center has different structures as shown in Fig. 4; parameters of the center appear to be determined mainly by the location of Fe^{3+} ion in its oxygen octahedron. Polar asymmetry of the location reverses together with the polarization of the sample, and the direction of the steady-state Stark shift stays the same with very close absolute magnitudes of the Stark coefficients. Different locations of the irregular Li^+ ion (nearest or next nearest oxygen octahedron to that which is occupied by an $\text{Fe}^{3+}[\text{Nb}]$ ion) cause only a small change in spectral position of the EPR line (compared to its width) in a zero E field for different directions of polarization of the sample: see Fig. 2(b).

The difference between the zero E field positions, δ , is comparable with the Stark shifts. The significantly different amplitudes of the slow spectral changes in the course of forward or backward repoling are due to the circumstance that in region 2 (Fig. 3) δ is *added* to the sum of the Stark shifts in the opposite domains but in region 4 it is *subtracted*: see arrows 2 and 4 in Fig. 2(b). This pictorial consideration clearly explains why the slow dynamics in Fig. 3(b) is a dominant feature during repoling from +3.5 to -3.5 kV, but barely seen during repoling in the opposite direction.

In conclusion, we would like to note that the observed properties of the Stark effect in a ferroelectric crystal appear to be quite general: ferroelectric-specific manifestations of the Stark effect may arise in *any* ferroelectric crystal when an external E field exceeds the coercive field thus causing a repoling of the sample. In ferroelectrics the effect becomes a more versatile phenomenon than in other solids. It is unlikely that this first example, $\text{LiNbO}_3\text{:Fe}$, covers all novel manifestations of the Stark effect which can be observed in ferroelectric crystals, a wide class of materials. There is nothing specific to EPR in the above reported results; these same phenomena may also be found in optical absorption, luminescence, or luminescence excitation spectroscopy. It is worth noting that optical irradiation may cause a significant decrease of the coercive fields (see [13] and references therein); therefore, in optical spectroscopy it may be easier to encounter ferroelectric-specific manifestations of the Stark effect than it is in EPR. There are impurities with Stark shifts comparable to or larger than the spectral line width [14], which may result in more fine effects than those reported here.

The authors gratefully acknowledge Professor S.E. Kapphan for providing samples and VTE processing in the University of Osnabrück, Germany and Dr. Gary Cook (Universal Technology Corporation/Air Force Research Laboratory) for useful discussions. This work was supported by RFBR (No. 06-02-17274-a) and CRDF (No. RPO-1385-ST-03).

- [1] A. A. Kaplyanskii, *J. Lumin.* **100**, 21 (2002).
- [2] P. F. Bordul, R. G. Norwood, D. H. Jundt, and M. M. Fejer, *J. Appl. Phys.* **71**, 875 (1992).
- [3] G. I. Malovichko, V. G. Grachev, O. F. Schirmer, and B. Faust, *J. Phys. Condens. Matter* **5**, 3971 (1993).
- [4] G. Malovichko, V. Grachev, and O. Schirmer, *Appl. Phys. B* **68**, 785 (1999).
- [5] S. A. Basun, V. E. Bursian, A. A. Kaplyanskii, A. G. Rzdobarin, L. S. Sochava, and D. R. Evans (to be published).
- [6] J. K. Jung, H. J. Kim, K. T. Han, and S. H. Choh, *Z. Naturforsch. A* **51**, 646 (1996).
- [7] A. P. Skvortsov, V. A. Trepakov, and L. Jastrabik, *J. Lumin.* **72-74**, 716 (1997).
- [8] D. L. Sun *et al.*, *Cryst. Res. Technol.* **39**, 511 (2004).
- [9] A. Savage, *J. Appl. Phys.* **37**, 3071 (1966).
- [10] M. Di Domenico and S. H. Wemple, *J. Appl. Phys.* **40**, 720 (1969).
- [11] H. Ishizuki, I. Shoji, and T. Taira, *Appl. Phys. Lett.* **82**, 4062 (2003).
- [12] *CRC Handbook of Chemistry and Physics*, edited by David R. Lide (CRC, Boca Raton, 2006); <http://www.webelements.com>.
- [13] M. C. Wengler, U. Heinemeyer, E. Soergel, and K. Buse, *J. Appl. Phys.* **98**, 064104 (2005).
- [14] V. Dierolf and C. Sandmann, *J. Lumin.* **125**, 67 (2007).